

Isotropization and Complexity of Decoupled Solutions in Self-interacting Brans-Dicke Gravity

M. Sharif ^{*} and Amal Majid [†]

Department of Mathematics, University of the Punjab,
Quaid-e-Azam Campus, Lahore-54590, Pakistan.

Abstract

The aim of this work is to formulate two new solutions by decoupling the field equations via a minimal geometric deformation in the context of self-interacting Brans-Dicke gravity. We introduce an extra source in the anisotropic fluid distribution to generate new analogs of existing solutions. The radial metric function is transformed to decouple the field equations into two sets such that each array corresponds to one source only. The system corresponding to the original matter distribution is specified by metric functions of well-behaved solutions. On the other hand, the second set is closed by imposing constraints on the additional matter source. For this purpose, we have applied the isotropization condition as well as vanishing complexity condition on the new source. Smooth matching of interior and exterior spacetimes at the junction provides values of the unknown constants. Interesting physical features of corresponding models are checked by employing the mass and radius of the star PSR J1614-2230. It is concluded that both extensions yield viable and stable models for certain values of the decoupling parameter.

Keywords: Brans-Dicke theory; Self-gravitating systems; Gravitational decoupling.

PACS: 04.50.Kd; 04.40.-b; 04.40.Dg

^{*}msharif.math@pu.edu.pk

[†]amalmajid89@gmail.com

1 Introduction

The theory of general relativity (GR) has played a significant role in understanding the mechanism and structure of the vast universe. The action of a theory encompasses the necessary elements describing a physical system and its motion. The addition of an extra degree of freedom in the form of a scalar, vector or tensor field modifies the action and yields alternative theories of gravity. In 1872, Mach presented a principle that referred to a relation between the inertia of a body and matter content in the universe. Later, Dirac's study of different physical constants alongside cosmological quantities indicated that the gravitational constant (G) has an underlying relationship with cosmic time [1]. Their results motivated Brans and Dicke [2] to modify GR by introducing a massless scalar field (σ) incorporating the effects of dynamic gravitational constant. This scalar-tensor theory (known as Brans-Dicke (BD) gravity) couples matter and scalar field through a coupling parameter (ω_{BD}) which may be assigned different values to describe various cosmic and astrophysical phenomena.

In cosmology, the inflationary model was proposed to overcome the flatness and horizon problems in the early cosmos. However, according to this model, the rapidly expanding universe fails to transition from the period of inflation into the next cosmological era. Although BD gravity has significant implications in the field of cosmology, it fails to successfully solve this problem (termed as the graceful exit problem). The BD coupling parameter must be less than 25 to adequately describe the inflationary era which disagrees with the statistical data. Moreover, in BD theory, the effect of scalar field decreases for higher values of ω_{BD} . Consequently, large values of the coupling parameter corresponding to weak field scenario [3] contradict the small values admissible in the era of cosmic inflation [4]. For the purpose of rectifying this discrepancy, a potential function ($V(\varrho)$) is introduced along with a massive scalar field (ϱ) leading to self-interacting BD (SBD) theory [5]. After this modification in BD gravity, all values of ω_{BD} greater than $\frac{3}{2}$ are permitted if the mass of the scalar field (m_ϱ) is more than $2 \times 10^{-25} GeV$ [6].

Researchers have employed various techniques to devise solutions describing different astrophysical phenomena under the influence of scalar field. Buchdahl [7] proposed that a family of vacuum solutions can be generated in BD gravity corresponding to static axially or spherically symmetric GR configurations. Bruckman and Kazes [8] investigated extremely dense fluid dis-

tributions described by a linear equation of state. They also showed that any GR solution with a proportional relationship between pressure and density can be used to construct an interior solution of BD field equations [9]. Singh and Rai [10] developed a scheme to obtain axially symmetric BD structure in presence of charge. Krori and Bhattacharjee [11] transformed the coordinate system to formulate a Demiański-type metric. The effect of scalar field on the rotation and other features of slowly as well as rapidly rotating neutron stars has been extensively discussed [12, 13]. Viable and stable anisotropic compact models corresponding to the MIT bag model equation of state have been computed in the presence of a massive scalar field [14]. Decoupled solutions via MGD have also been obtained in the background of SBD and other modifications of GR [15].

The vast network of interconnected galactic clusters and stars contains clues regarding the history of our existence and ultimately the universe. By analyzing the age and evolution of gaseous stars and their compact remnants, astrophysicists have gained important information that can prove beneficial in revealing the mysterious nature of the cosmic mechanism. For this purpose, researchers have given considerable attention to the mathematical modeling of stellar structures by computing solutions of the field equations. The field equations provide the necessary connection between matter and geometry of large-scale structures but their non-linearity complicates the extraction of well-behaved solutions representing realistic physical structures. Schwarzschild [16] resolved this problem by considering a simple spherical object. However, cosmic structures are complex systems with a large number of state determinants. Therefore, researchers are still attempting to devise different methods that produce viable stellar models.

In this regard, Ovalle [17] extended the well-known Tolman IV solution by adding a new source. According to Ovalle's technique, the system of field equations incorporating the effects of seed and additional sources are decoupled into two arrays via a minimal geometric deformation (MGD) in the radial coordinate. The first array includes the energy-momentum tensor corresponding to the original fluid distribution only while the influence of extra source is exclusively described by the second system. The known solution specifies the first set (leading to reduced degrees of freedom) while the second system is closed by applying a constraint on the additional matter source. A linear combination of the solutions corresponding to each system provides a new solution of the entire system. According to this approach, the coexisting sources do not exchange energy and are individually conserved.

The scheme of decoupling via MGD has been extended by introducing linear deformations in radial as well as temporal metric components [18].

The decoupling technique via MGD has facilitated the extraction of many astrophysical and cosmological solutions. Ovalle [19] first applied MGD approach to accommodate the extra spatial dimension in the Randall-Sundrum braneworld. Later, he also used this technique to compute an analog of Tolman IV solution in braneworld [20]. Casadio et al. [21] introduced an extension of MGD in context of Randall-Sundrum braneworld to obtain a modified Schwarzschild geometry. This technique has been generally employed to construct anisotropic versions of different isotropic solutions (Tolman IV [22], Durgapal-Fuloria [23], Heintzmann [24], Krori-Barua [25]) in general relativity (GR). Panotopoulos et al. [26] applied the technique of MGD to a cloud of strings. Gabbanelli et al. [27] reconstructed the Schwarzschild solution with cosmological constant via decoupling and obtained an extension with non-uniform density. This approach has been successfully applied in (2+1)-dimensional spacetime as well [28, 29].

Casadio et al. [30] used decoupling to control the anisotropy and complexity of a static self-gravitating system. Hensh and Stuchlik [31] deformed the radial metric function of Tolman VII spacetime to evaluate its anisotropic version. Singh et al. [32] developed isotropic solutions using Karmarkar's condition and then extended them to the anisotropic domain via MGD. Viable anisotropic extensions of a cloud of strings have also been obtained by employing the same technique [33]. Cedeño and Contreras [34] showed that the decoupling approach is also applicable in the field of cosmology by deforming FLRW and Kantowski-Sachs spacetimes. Tello-Ortiz et al. [35] extended the Durgapal IV solution to anisotropic domain via MGD. Deformations of Dirac as well as Yang-Mills-Dirac configurations have also been obtained by deforming the radial metric function [36, 37]. Axially symmetric Kerr and Kerr-Newman spacetimes were also successfully extended via this scheme [38]. Recently, Contreras and Fuenmayor [39] analyzed the stability of static spheres via gravitational cracking in the background of decoupling. Sultana [40] showed the applicability of decoupling through MGD in higher order theories as well.

In this paper, we show that the decoupling via the MGD scheme can be adopted to control certain physical features of static spherical self-gravitating systems in the context of SBD gravity. We compute two new solutions by governing the anisotropy as well as complexity of the matter distribution. The paper is arranged in the following format. The anisotropic field equations

involving the additional source are constructed in the next section. The radial deformation is applied to decouple the field equations in section 3. In section 4, we construct new versions of well-known ansatz and inspect them graphically. A summary of the main results is presented in the last section.

2 Self-interacting Brans-Dicke Theory

Replacing the gravitational constant in GR by a massive scalar field leads to the action (in relativistic units) of SBD gravity given as

$$\mathcal{S} = \int \sqrt{-g} (\mathfrak{R}\varrho - \frac{\omega_{BD}}{\varrho} \nabla^\gamma \varrho \nabla_\gamma \varrho - V(\varrho) + L_m + \eta L_\Theta) d^4x, \quad (1)$$

where the Lagrangians of matter and additional sources are denoted by L_m and L_Θ , respectively. The influence of the extra source (Θ) is determined by the decoupling parameter η . Moreover, g and \mathfrak{R} denote the determinant of the metric tensor ($g_{\gamma\delta}$) and Ricci scalar, respectively. The field and wave equations in SBD gravity, respectively read

$$G_{\gamma\delta} = \mathfrak{R}_{\gamma\delta} - \frac{1}{2} g_{\gamma\delta} \mathfrak{R} = T_{\gamma\delta}^{(\text{eff})} = \frac{1}{\varrho} (T_{\gamma\delta}^{(m)} + \eta \Theta_{\gamma\delta} + T_{\gamma\delta}^e), \quad (2)$$

$$\square \varrho = \frac{1}{2\omega_{BD} + 3} \left(T^{(m)} + \eta \Theta + \left(\varrho \frac{dV(\varrho)}{d\varrho} - 2V(\varrho) \right) \right). \quad (3)$$

Here, $T_{\gamma\delta}^{(m)}$ corresponds to the energy-momentum tensor of the original fluid distribution while the impact of the scalar field on salient characteristics of the compact structure is measured through the tensor

$$T_{\gamma\delta}^e = \varrho_{,\gamma;\delta} - g_{\gamma\delta} \square \varrho + \frac{\omega_{BD}}{\varrho} \left(\varrho_{,\gamma} \varrho_{,\delta} - \frac{g_{\gamma\delta} \varrho_{,\alpha} \varrho^{,\alpha}}{2} \right) - \frac{V(\varrho) g_{\gamma\delta}}{2}, \quad (4)$$

where \square is the d'Alembertian operator, $g^{\gamma\delta} T_{\gamma\delta}^{(m)} = T^{(m)}$ and $g^{\gamma\delta} \Theta_{\gamma\delta}^{(m)} = \Theta$. The two matter sources are present in a static spherical region covered by a three-dimensional hypersurface (Σ) and described by the line element

$$ds^2 = e^{\phi_1(r)} dt^2 - e^{\phi_2(r)} dr^2 - r^2 d\theta^2 - r^2 \sin^2 \theta d\varphi^2. \quad (5)$$

We assume that the seed source is anisotropic in nature whose energy and momentum are represented by the following tensor

$$T_{\gamma\delta}^{(m)} = (\rho + p_\perp) v_\gamma v_\delta - p_\perp g_{\gamma\delta} + (p_r - p_\perp) s_\gamma s_\delta, \quad (6)$$

where ρ , p_r and p_\perp denote the energy density, radial and transverse components of pressure, respectively. Moreover, $v_\gamma = (e^{\frac{\phi_1}{2}}, 0, 0, 0)$ is the four-velocity while $s_\gamma = (0, -e^{\frac{\phi_2}{2}}, 0, 0)$ corresponds to the radial four-vector. The effective energy-momentum tensor, incorporating the effects of scalar field and additional source, obeys the conservation law. The field equations (2) take the following form for metric (5) in the presence of scalar field

$$\frac{1}{r^2} - e^{-\phi_2} \left(\frac{1}{r^2} - \frac{\phi_2'}{r} \right) - \frac{T_0^{0\varrho}}{\varrho} = \frac{1}{\varrho} (\rho + \eta \Theta_0^0), \quad (7)$$

$$-\frac{1}{r^2} + e^{-\phi_2} \left(\frac{1}{r^2} + \frac{\phi_1'}{r} \right) + \frac{T_1^{1\varrho}}{\varrho} = \frac{1}{\varrho} (p_r - \eta \Theta_1^1), \quad (8)$$

$$\frac{e^{-\phi_2}}{4} \left(2\phi_1'' + \phi_1'^2 - \phi_2'\phi_1' + 2\frac{\phi_1' - \phi_2'}{r} \right) + \frac{T_2^{2\varrho}}{\varrho} = \frac{1}{\varrho} (p_\perp - \eta \Theta_2^2), \quad (9)$$

where

$$\begin{aligned} T_0^{0\varrho} &= e^{-\phi_2} \left[\varrho'' + \left(\frac{2}{r} - \frac{\phi_2'}{2} \right) \varrho' + \frac{\omega_{BD}}{2\varrho} \varrho'^2 - e^{\phi_2} \frac{V(\varrho)}{2} \right], \\ T_1^{1\varrho} &= e^{-\phi_2} \left[\left(\frac{2}{r} + \frac{\phi_1'}{2} \right) \varrho' - \frac{\omega_{BD}}{2\varrho} \varrho'^2 - e^{\phi_2} \frac{V(\varrho)}{2} \right], \\ T_2^{2\varrho} &= e^{-\phi_2} \left[\varrho'' + \left(\frac{1}{r} - \frac{\phi_2'}{2} + \frac{\phi_1'}{2} \right) \varrho' + \frac{\omega_{BD}}{2\varrho} \varrho'^2 - e^{\phi_2} \frac{V(\varrho)}{2} \right]. \end{aligned}$$

Here, differentiation with respect to r is indicated by $'$. Moreover, the signature is included in the unknown components of Θ_δ^γ . Furthermore, the wave equation corresponding to the current scenario is expressed as

$$\begin{aligned} \square\varrho &= -e^{-\phi_2} \left[\left(\frac{2}{r} - \frac{\phi_2'}{2} + \frac{\phi_1'}{2} \right) \varrho' + \varrho'' \right] \\ &= \frac{1}{3 + 2\omega_{BD}} \left[\eta\Theta + T^{(m)} + \left(\varrho \frac{dV(\varrho)}{d\varrho} - 2V(\varrho) \right) \right]. \quad (10) \end{aligned}$$

Various cosmological and astrophysical models have been developed corresponding to different forms of self-interacting potentials [41]. The specific form of potential is unknown but it has been assumed that at high temperatures the potential is proportional to ϖ^2 [42]. Furthermore, Quiros [43] showed that the de Sitter solution in general relativity arises in the SBD

theory for the quadratic potential ($V(\varpi) = m^2\varpi^2$, where m is coupled to the mass of the scalar field) only. We proceed by assuming that

$$V(\varpi) = \frac{1}{2}m_\varpi^2\varpi^2,$$

where $m_\varrho = 0.01$ as the weak field observations are satisfied in SBD theory for $m_\varrho > 10^{-4}$ (in dimensionless units). Note that the combination $(\varpi \frac{dV(\varpi)}{d\varpi} - 2V(\varpi))$ in Eq.(10) vanishes for the chosen potential function which simplifies the mathematical calculations. This form of potential function has been previously considered for different cosmic scenarios [13, 42, 44]. It is noted that the inclusion of the source Θ in the field equations has increased the number of unknowns: $\phi_1, \phi_2, \rho, p_r, p_\perp, \Theta_0^0, \Theta_1^1, \Theta_2^2, \varrho$.

3 Gravitational Decoupling

The scheme of decoupling via MGD transforms the radial metric component as

$$e^{-\phi_2(r)} \mapsto \lambda(r) + \eta\mu(r), \quad (11)$$

while the temporal metric potential is not deformed. The modification in the radial component is controlled by the deformation function $\mu(r)$. Moreover, the linear mapping does not disturb the symmetry of the sphere. As a consequence of applying the transformation, the complicated field equations yield two arrays. The first set (for $\eta = 0$) encodes the influence of the anisotropic seed source as

$$\begin{aligned} \rho &= -\frac{1}{2r^2\varrho(r)}[r^2\omega_{BD}\lambda(r)\varrho'^2 - r^2\varrho(r)V(\varrho) + r\varrho(r)(r\lambda'(r)\varrho'(r) + 2r\lambda\varrho'' \\ &+ 4\lambda(r)\varrho'(r)) + 2\varrho^2(r)(r\lambda'(r) + \lambda(r) - 1)], \end{aligned} \quad (12)$$

$$\begin{aligned} p_r &= \frac{1}{r^2}[\varrho(r)(r\lambda(r)\phi_1'(r) + \lambda(r) - 1)] + \frac{1}{2r\varrho(r)}[\lambda(r)\varrho'(r)(\varrho(r)(r\phi_1'(r) + 4) \\ &- r\omega_{BD}\varrho'(r))] - \frac{V(\varrho)}{2}, \end{aligned} \quad (13)$$

$$\begin{aligned} p_\perp &= \frac{1}{4r\varrho(r)}[\varrho(r)\lambda'(r)(\varrho(r)(r\phi_1'(r) + 2) + 2r\varrho'(r)) + \lambda(r)(2\varrho(r)\varrho'(r) \\ &\times ((r\phi_1'(r) + 2) + 2r\varrho''(r)) + \varrho^2(r)(2r\phi_1''(r) + r\phi_1'^2(r) + 2\phi_1'(r))] \end{aligned}$$

$$+ 2r\omega_{BD}\varrho'^2(r) - 2r\varrho(r)V(\varrho)]. \quad (14)$$

The conservation equation of the seed matter distribution is obtained as

$$T_1^{1'(\text{eff})} - \frac{\phi_1'(r)}{2}(T_0^{0(\text{eff})} - T_1^{1(\text{eff})}) - \frac{2}{r}(T_2^{2(\text{eff})} - T_1^{1(\text{eff})}) = 0. \quad (15)$$

The characteristics of the additional source are exclusively included in the second set as

$$\begin{aligned} \Theta_0^0 &= \frac{-1}{2r^2\varrho(r)}[r\varrho(r)\mu'(r)(r\varrho'(r) + 2\varrho(r)) + \mu(r)(r^2\omega_{BD}\varrho'^2(r) + 2r\varrho(r) \\ &\times (r\varrho''(r) + 2\varrho'(r)) + 2\varrho^2(r))], \end{aligned} \quad (16)$$

$$\begin{aligned} \Theta_1^1 &= \frac{-1}{2r^2\varrho(r)}[\mu(r)(-r^2\omega_{BD}\varrho'^2(r) + r\varrho(r)(r\phi_1'(r) + 4)\varrho'(r) + 2\varrho^2(r) \\ &\times (r\phi_1'(r) + 1))], \end{aligned} \quad (17)$$

$$\begin{aligned} \Theta_2^2 &= \frac{-1}{4\varrho(r)}[2\varrho(r)(r\mu'(r)\varrho'(r) + \mu(r)((r\phi_1'(r) + 2)\varrho'(r) + 2r\varrho''(r))) \\ &+ \varrho^2(r)(\mu'(r)(r\phi_1'(r) + 2) + \mu(r)(2r\phi_1''(r) + r\phi_1'^2(r) + 2\phi_1'(r))) \\ &+ 2r\omega_{BD}\mu(r)\varrho'^2(r)]. \end{aligned} \quad (18)$$

The conservation equation associated with the above system is

$$\Theta_1^{1'(\text{eff})} - \frac{\phi_1'(r)}{2}(\Theta_0^{0(\text{eff})} - \Theta_1^{1(\text{eff})}) - \frac{2}{r}(\Theta_2^{2(\text{eff})} - \Theta_1^{1(\text{eff})}) = 0, \quad (19)$$

where

$$\begin{aligned} \Theta_0^{0(\text{eff})} &= \frac{1}{\varrho} \left(\Theta_0^0 + \frac{1}{2}\mu'(r)\varrho'(r) + \mu(r)\varrho''(r) + \frac{\omega_{BD}\mu(r)\varrho'^2(r)}{2\varrho(r)} + \frac{2\mu(r)\varrho'}{r} \right), \\ \Theta_1^{1(\text{eff})} &= \frac{1}{\varrho} \left(\Theta_1^1 + \frac{1}{2}\mu(r)\phi_1'(r)\varrho'(r) - \frac{\omega_{BD}\mu(r)\varrho'^2(r)}{2\varrho(r)} + \frac{2\mu(r)\varrho'(r)}{r} \right), \\ \Theta_2^{2(\text{eff})} &= \frac{1}{\varrho} \left(\Theta_2^2 + \frac{1}{2}\mu'(r)\varrho'(r) + \frac{1}{2}\mu(r)\phi_1'(r)\varrho'(r) + \mu(r)\varrho''(r) \right. \\ &\left. + \frac{\omega_{BD}\mu(r)\varrho'^2(r)}{2\varrho(r)} + \frac{\mu(r)\varrho'(r)}{r} \right). \end{aligned}$$

The MGD technique prohibits the exchange of energy between the additional and original fluid distributions. Thus, the two sources are conserved individually as indicated by Eqs.(15) and (19). The number of unknown variables

decreases if a well-behaved solution is assumed for Eqs.(12)-(14). On the other hand, a constraint on Θ -sector determines the deformation function and specifies the second set. Finally, combining these solutions generates new ansatz with the following energy density and pressure components

$$\begin{aligned} \rho &= \frac{-1}{2r^2\varrho(r)}[r\varrho(r)(r\varrho'(r)(\eta\mu'(r) + \lambda'(r)) + 2\eta\mu(r)(r\varrho''(r) + 2\varrho'(r)) \\ &+ 2\lambda(r)(r\varrho''(r) + 2\varrho'(r))) + 2\varrho^2(r)(\eta r\mu'(r) + \eta\mu(r) + r\lambda'(r) + \lambda(r) \\ &- 1) + r^2\omega_{BD}\varrho'^2(r)(\eta\mu(r) + \lambda(r)) - r^2\varrho(r)V(\varrho)], \end{aligned} \quad (20)$$

$$\begin{aligned} p_r &= \frac{1}{2r^2\varrho}[r^2\omega_{BD}\varrho'^2(r)(\eta\mu(r) - \lambda(r)) - r\varrho(r)(r\phi_1'(r) + 4)\varrho'(r)(\eta\mu(r) \\ &- \lambda(r)) + 2\varrho^2(r)(-\mu(r)(\eta + \eta r\phi_1'(r)) + r\lambda(r)\phi_1'(r) + \lambda(r) - 1) \\ &- r^2\varrho(r)V(\varrho)], \end{aligned} \quad (21)$$

$$\begin{aligned} p_{\perp} &= \frac{1}{4r\varrho(r)}[-2\varrho(r)(r\varrho'(r)(\eta\mu'(r) - \lambda'(r)) + \eta\mu(r)((r\phi_1'(r) + 2)\varrho'(r) \\ &+ 2r\varrho''(r)) - \lambda(r)((r\phi_1'(r) + 2)\varrho'(r) + 2r\varrho''(r))) - \varrho^2(r)(\eta\mu'(r)(r\phi_1'(r) \\ &+ 2) - \eta\mu(2r\phi_1''(r) + r\phi_1'^2(r) + 2\phi_1'(r)) + 2r\lambda(r)\phi_1''(r) + r\phi_1'(r)\lambda'(r) \\ &+ r\lambda(r)\phi_1'^2(r) + 2\lambda(r)\phi_1'(r) + 2\lambda'(r)) + 2r\omega_{BD}\varrho'^2(r)(\lambda(r) - \eta\mu(r)) \\ &- 2r\varrho(r)V(\varrho)]. \end{aligned} \quad (22)$$

4 Decoupled Solutions

In this section, we impose constraints on the new source to develop two solutions representing self-gravitating systems in the presence of massive scalar field. We graphically analyze the generated solutions and inspect their important features.

4.1 Solution I

For the first solution, we employ the following ansatz to determine the set related to anisotropic seed source

$$\phi_1(r) = \ln\left(B^2\left(\frac{r^2}{A^2} + 1\right)\right), \quad (23)$$

$$\lambda(r) = \left(\frac{A^2 + r^2}{A^2 + 3r^2}\right), \quad (24)$$

where A and B are constants. These metric potentials belong to a class of solutions that determine the gravitational field in a cluster of particles following randomly oriented circular orbits [45]. Moreover, this spacetime has been previously used to construct decoupled solutions in GR [30]. The surface of the compact object is the junction between the interior and exterior spacetimes. In order to avoid any singularity, the anisotropic interior must smoothly connect with the vacuum Schwarzschild metric defined as

$$ds^2 = \frac{r-2M}{r} dt^2 - \frac{r}{r-2M} dr^2 - r^2 d\theta^2 - r^2 \sin^2 \theta d\varphi^2, \quad (25)$$

where M denotes the mass. The form of scalar field in the vacuum exterior has been determined via the procedure used in [8]. The conditions

$$\begin{aligned} (g_{\gamma\delta}^-)_{\Sigma} &= (g_{\gamma\delta}^+)_{\Sigma}, & (p_r)_{\Sigma} &= 0, \\ (\varrho^-(r))_{\Sigma} &= (\varrho^+(r))_{\Sigma}, & (\varrho'^-(r))_{\Sigma} &= (\varrho'^+(r))_{\Sigma}, \end{aligned}$$

ensure the smooth matching at the hypersurface ($\Sigma : r = R$, R is the radius of the celestial object). The values of unknown constants are obtained through these conditions as

$$A = \frac{\sqrt{R^2(R-3M)}}{\sqrt{M}}, \quad (26)$$

$$B = \frac{\sqrt{R-2M}}{\sqrt{\frac{MR}{R-3M} + R}}, \quad (27)$$

where M and R are specified by employing the mass and radius of PSR J1614-2230 ($M = 1.97M_{\odot}$ and $R = 11.29km$). The field equations (20)-(22) take the following form corresponding to Eqs.(23) and (24)

$$\begin{aligned} \rho &= - \left(2r^2 (A^2 + 3r^2)^2 \varrho \right)^{-1} \left(2\varrho^2 \left(r \left(\eta (A^2 + 3r^2)^2 \mu' - 6r (A^2 + r^2) \right) \right. \right. \\ &+ \left. \eta (A^2 + 3r^2)^2 \mu(r) \right) + r^2 \omega_{BD} (A^2 + 3r^2) \varrho'^2(r) \left(\eta (A^2 + 3r^2) \mu(r) \right. \\ &+ \left. A^2 + r^2 \right) - r^2 (A^2 + 3r^2)^2 \varrho(r) V(\varrho) + r \varrho(r) \left(2r (A^2 + 3r^2) \varrho''(r) \right. \\ &\times \left. \left(\eta (A^2 + 3r^2) \mu(r) + A^2 + r^2 \right) + \varrho'(r) \left(\eta r (A^2 + 3r^2)^2 \mu'(r) \right. \right. \\ &+ \left. \left. 4\eta (A^2 + 3r^2)^2 \mu(r) + 4(A^4 + 3A^2 r^2 + 3r^4) \right) \right), \end{aligned}$$

$$\begin{aligned}
p_r &= \frac{-1}{2r\varrho} \left(\varrho' \left(\frac{A^2 + r^2}{A^2 + 3r^2} + \eta\mu \right) \left(\left(-\frac{2r^2}{A^2 + r^2} - 4 \right) \varrho(r) + r\omega_{BD}\varrho' \right) \right) \\
&+ \frac{\eta(A^2 + 3r^2)\mu(r)\varrho(r)}{r^2(A^2 + r^2)} - \frac{V(\varrho)}{2}, \\
p_\perp &= \left(2r(A^2 + r^2)^2 (A^2 + 3r^2)^2 \varrho(r) \right)^{-1} \left(\varrho^2(r) \left((A^2 + r^2) (\eta(A^2 + 2r^2) \right. \right. \\
&\times \left. \left. (A^2 + 3r^2)^2 \mu' + 6r^3 (A^2 + r^2) \right) + 2\eta r (2A^2 + r^2) (A^2 + 3r^2)^2 \mu(r) \right) \\
&+ r\omega_{BD} (A^2 + r^2)^2 (A^2 + 3r^2)^2 \varrho'^2 (\eta(A^2 + 3r^2)\mu(r) + A^2 + r^2) \\
&+ (A^2 + r^2) \varrho(r) \left(\varrho'(r) \left(2\eta(A^2 + 2r^2) (A^2 + 3r^2)^2 \mu(r) + (A^2 + r^2) \right. \right. \\
&\times \left. \left. \left(\eta r (A^2 + 3r^2)^2 \mu' + 2(A^4 + 3A^2 r^2 + 6r^4) \right) \right) + 2r\varrho'' (A^4 + 4A^2 r^2 \right. \\
&+ \left. 3r^4) (\eta(A^2 + 3r^2)\mu + A^2 + r^2) \right) - r(A^4 + 4A^2 r^2 + 3r^4)^2 \varrho V(\varrho).
\end{aligned}$$

The total anisotropy of the system under the influence of scalar field is

$$\Delta = (p_\perp - \eta\Theta_2^2) - (p_r - \eta\Theta_1^1) = (p_\perp - p_r) + \eta(\Theta_1^1 - \Theta_2^2), \quad (28)$$

We solve Eqs.(16)-(18) in the current setup by assuming that the addition of new source converts the anisotropic structure into an isotropic system for $\eta = 1$, i.e., Δ reduces to zero for $\eta = 1$ yielding

$$p_\perp - p_r = -(\Theta_1^1 - \Theta_2^2). \quad (29)$$

Recently, Casadio et al. [30] utilized the above condition to isotropize an anisotropic source through decoupling. The isotropization condition corresponding to the metric functions in Eqs.(23) and (24) takes the form

$$\begin{aligned}
&\left(r\varrho(A^2 + r^2)(A^2 + 3r^2) \right)^{-1} \left(2r^2\omega_{BD}(A^2 + 3r^2)(A^2 + r^2)^2 \left((A^2 \right. \right. \\
&+ \left. \left. 3r^2)\mu + A^2 + r^2 \right) \varrho'^2 + r(A^2 + r^2)^2 \varrho \left(2r(A^2 + 3r^2) \left((A^2 + 3r^2)\mu \right. \right. \right. \\
&+ \left. \left. A^2 + r^2 \right) \varrho''(r) + \varrho'(r) \left(r(A^2 + 3r^2)^2 \mu'(r) - 2(A^2 + 3r^2)^2 \mu(r) \right. \right. \\
&- \left. \left. 2(A^4 + 6A^2 r^2 + 3r^4) \right) \right) + \varrho^2 \left(r(A^2 + r^2) \left((A^2 + 2r^2)(A^2 + 3r^2)^2 \mu' \right. \right. \\
&+ \left. \left. 6r^3(A^2 + r^2) \right) - 2(A^2 + 3r^2)^2 (A^4 + 2A^2 r^2 + 2r^4) \mu \right) = 0. \quad (30)
\end{aligned}$$

The deformation function is evaluated by numerically solving the above equation alongside Eq.(10) for $\varrho(0) = 0.1$ and $\mu(0) = 0$. Further, we graphically

Table 1: Values of physical parameters in solution I corresponding to $\eta = 0.2, 0.5, 1$.

	$\eta = 0.2$	$\eta = 0.5$	$\eta = 1$
ω_{BD}	-1.4	6	1
$\rho_c (gm/cm^3)$	4.506×10^{15}	7.721×10^{15}	4.385×10^{15}
$\rho_s (gm/cm^3)$	4.883×10^{14}	1.171×10^{15}	2.448×10^{14}
$p_c (dyne/cm^2)$	1.3×10^{36}	4.148×10^{36}	7.465×10^{36}
Z_s	0.026	0.042	0.0218

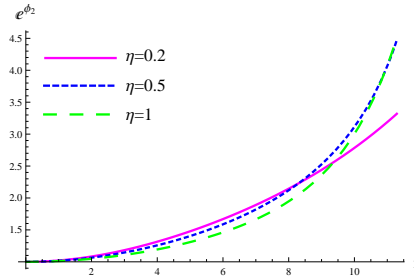


Figure 1: Behavior of deformed radial metric potential for solution I.

analyze the constructed solution for $\eta = 0.2, 0.5, 1$. The corresponding values of coupling parameter are mentioned in Table 1 where the quantities with subscripts c and s are calculated at the center and surface of the star, respectively. Moreover, the constant A does not change after the transformation while B cannot be determined. Therefore, we choose the value of B as given in Eq.(27). The transformed radial metric function is monotonically increasing and free from singularity as shown in Figure 1. Compact objects are the most dense at the center leading to maximum pressure at $r = 0$. Moreover, the radial pressure always approaches to zero near the boundary of the cosmic structure. Figure 2 indicates that the matter variables are consistent with the required criteria. The object becomes more dense as the value of decoupling parameter increases from 0.2 to 0.5 but then decreases for $\eta = 1$. However, pressure components follow the opposite trend, i.e., radial/tangential pressure decreases when value of η increases from 0.2 to 0.5 but then slightly increases for $\eta = 1$. It is noted that anisotropy is zero at the center for $\eta = 0.2, 0.5$ whereas it vanishes for $\eta = 1$ as required.

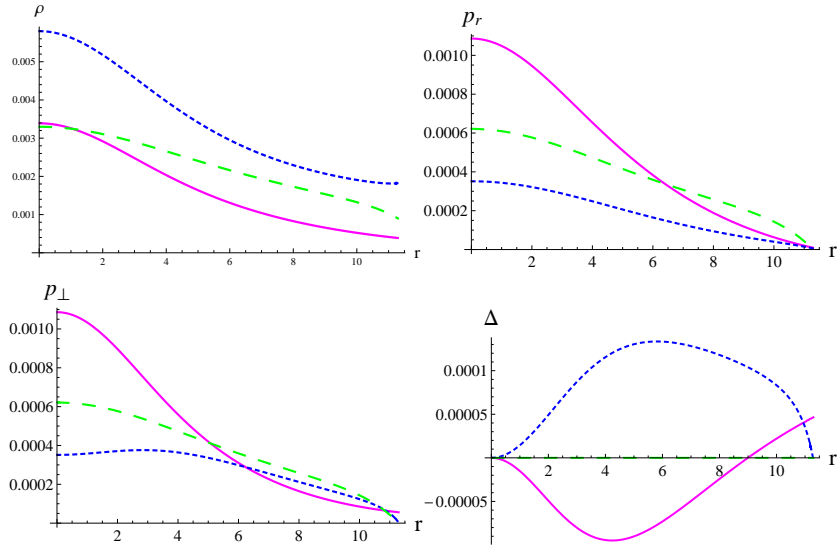


Figure 2: Behavior of ρ , p_r , p_\perp (in km^{-2}) and Δ for solution I.

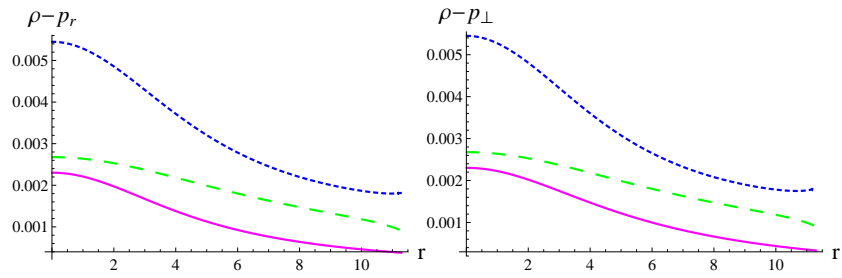


Figure 3: DEC for solution I.

The astrophysical systems composed of normal matter comply with four energy bounds listed as [46]

$$\begin{aligned}
&\text{null energy condition: } \rho + p_r \geq 0, \quad \rho + p_\perp \geq 0, \\
&\text{weak energy condition: } \rho \geq 0, \quad \rho + p_r \geq 0, \quad \rho + p_\perp \geq 0, \\
&\text{strong energy condition: } \rho + p_r + 2p_\perp \geq 0, \\
&\text{dominant energy condition: } \rho - p_r \geq 0, \quad \rho - p_\perp \geq 0.
\end{aligned}$$

These conditions ensure that the fluid distribution inside the static sphere is physically viable. The new structure satisfies the first three energy bounds as the density and pressure are non-negative throughout the interior (refer to Figure 2). Further, the graphical representations of $\rho - p_r$ and $\rho - p_\perp$ in Figure 3 indicate the fulfilment of dominant energy condition as well. Thus, the matter distribution within spherical structure is viable for the considered values of η .

In order to compute the mass of the spherical distribution, we numerically solve the differential equation

$$\frac{dm(r)}{dr} = \frac{1}{2}r^2\rho, \tag{31}$$

subject to the initial condition $m(0) = 0$. The compactness of the celestial object depends on the arrangement of composite particles. Highly compact objects have tightly packed particles as compared to structures with less compactness. The mass to radius ratio (also known as compactness factor ($u(r)$)) gauges the compactness of a cosmic object. According to Buchdahl's study [47], the compactness of a spherical structure obeys the limit $u(r) < \frac{4}{9}$. Further, the compactness of an astrophysical object influences the wavelength of nearby electromagnetic radiations. The waves deviate from the straight path due to the strong gravitational field of extremely dense structures. The redshift in electromagnetic radiation is measured as

$$Z(r) = \frac{1 - \sqrt{1 - 2u}}{\sqrt{1 - 2u}},$$

which should not exceed the values 2 and 5.211 corresponding to isotropic [47] and anisotropic configurations [48], respectively. The plots in Figure 4 indicate that the isotropic spherical system is more massive and compact as compared to the anisotropic analog. Consequently, it exerts a stronger

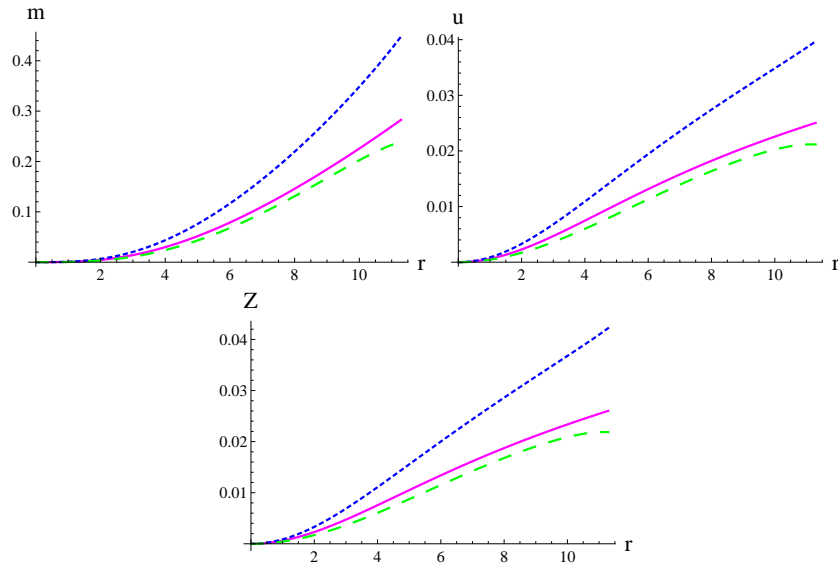


Figure 4: Behavior of m , u and Z corresponding to solution I.

gravitational field leading to higher redshifts. It is worthwhile to mention here that the compactness and redshift parameters lie within their respective admissible ranges.

We check the stability of the current setup by calculating the radial ($v_r^2 = \frac{dp_r}{d\rho}$) and tangential ($v_\perp^2 = \frac{dp_\perp}{d\rho}$) speeds of sound traveling through the considered medium. Sound wave must travel at a speed less than that of light to maintain causality, i.e., v_r^2 and v_\perp^2 must lie within the interval $(0, 1)$. Figure 5 illustrates that the celestial structure is unstable for $\eta = 0.2$ as $v_\perp^2 < 0$. However, the system attains stability when η increases. Herrera's cracking concept is an additional tool to inspect the stability of the system. This criterion is fulfilled when the components of sound speed satisfy the inequality $0 < |v_\perp^2 - v_r^2| < 1$. The static sphere is consistent with this criterion for lower as well as higher values of η as shown in Figure 5.

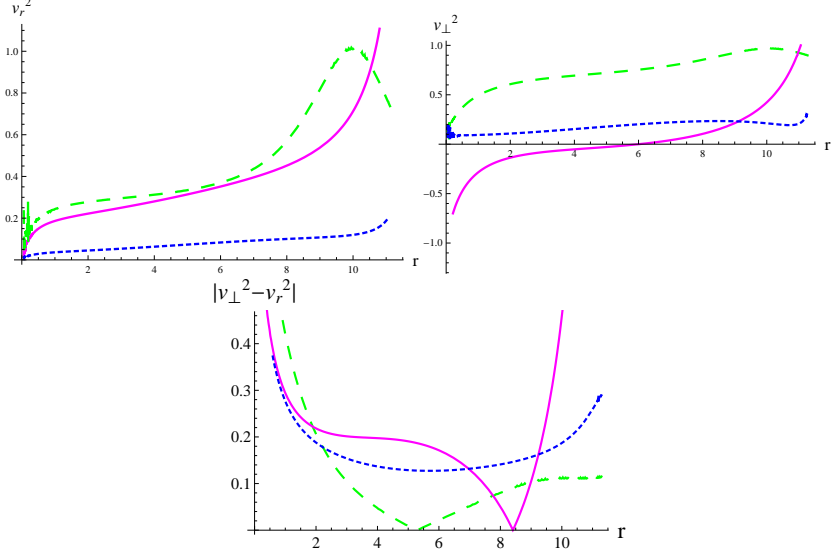


Figure 5: Plots of radial/tangential velocities and $|v_{\perp}^2 - v_r^2|$ of solution I.

4.2 Solution II

In order to formulate the second solution, we specify Eqs.(12)-(14) via the metric potentials of Tolman IV solution given as [49]

$$\phi_1(r) = \ln \left(b^2 \left(\frac{r^2}{a^2} + 1 \right) \right), \quad (32)$$

$$\lambda(r) = \left(\frac{\left(\frac{r^2}{a^2} + 1 \right) \left(1 - \frac{r^2}{f^2} \right)}{\frac{2r^2}{a^2} + 1} \right), \quad (33)$$

where the unknown constants a , b and f are determined via a singularity-free junction with Schwarzschild vacuum solution as

$$a^2 = -\frac{R^2 (M (28R - 2Rh + R^2h) - 2M^2(12 - \omega_{BD}) - 8R^2)}{hR(R - 2M) + 2M^2\omega_{BD}}, \quad (34)$$

$$b^2 = \frac{(3hR^2 + 6M^2(\omega_{BD} + 12) - 6M(Rh + 10R) + 8R^2)(R - 2M)}{2R(hR^2 + 2M^2(\omega_{BD} + 12) - 2M(Rh + 11R) + 4R^2)}, \quad (35)$$

$$f^2 = (m_e^4 R^6 + M^2 (2h(\omega_{BD} + 12 + 4m_e^4 R^4) + 4R^2h + 8(\omega_{BD} + 12)))$$

$$- 4M (m_e^4 R^5 + 6Rh + 16R)^{-1} (4R^3 (3M - 2R) (h + 4)). \quad (36)$$

where $h = m_e^2 R^2 \sqrt{1 - \frac{2M}{R}}$. The field equations related to the considered setup take the form

$$\begin{aligned} \rho &= \left(2f^2 r^2 (a^2 + 2r^2)^2 \varrho \right)^{-1} \left(r^2 \omega_{BD} (a^2 + 2r^2) \varrho'^2 ((a^2 + r^2) (r^2 - f^2) \right. \\ &- \eta f^2 (a^2 + 2r^2) \mu(r)) + f^2 r^2 (a^2 + 2r^2)^2 \varrho(r) V(\varrho) + 2\varrho^2 (r (r (3a^4 \\ &+ 3a^2 f^2 + 7a^2 r^2 + 2f^2 r^2 + 6r^4) - \eta f^2 (a^2 + 2r^2)^2 \mu'(r)) - \eta f^2 (a^2 \\ &+ 2r^2)^2 \mu(r)) - r \varrho(r) (2r (a^2 + 2r^2) \varrho''(r) (\eta f^2 (a^2 + 2r^2) \mu(r) \\ &+ (a^2 + r^2) (f^2 - r^2)) + \varrho'(r) (\eta f^2 r (a^2 + 2r^2)^2 \mu'(r) + 4\eta f^2 (a^2 \\ &+ 2r^2)^2 \mu + 2(a^4 (2f^2 - 3r^2) + a^2 (5f^2 r^2 - 8r^4) + 4f^2 r^4 - 6r^6))) \Big), \\ p_r &= - \frac{\varrho'(r) \left(\frac{(a^2+r^2)(f^2-r^2)}{f^2(a^2+2r^2)} + \eta \mu(r) \right) \left(r \omega_{BD} \varrho'(r) - \frac{2(2a^2+3r^2)\varrho(r)}{a^2+r^2} \right)}{2r \varrho(r)} \\ &+ \frac{\varrho(r)}{r^2} \left(\frac{(a^2 + 3r^2) \left(\frac{(a^2+r^2)(f^2-r^2)}{f^2(a^2+2r^2)} + \eta \mu(r) \right)}{a^2 + r^2} - 1 \right) - \frac{V(\varrho)}{2}, \\ p_\perp &= \left(2f^2 r (a^2 + r^2)^2 (a^2 + 2r^2)^2 \varrho \right)^{-1} \left(r \omega_{BD} (a^2 + r^2)^2 (a^2 + 2r^2) \varrho'^2 \right. \\ &\times (\eta f^2 (a^2 + 2r^2) \mu + (a^2 + r^2) (f^2 - r^2)) - (a^2 + 2r^2) \varrho^2 ((a^2 + r^2) \\ &\times (2r (a^2 + r^2) (a^2 - f^2 + 3r^2) - \eta f^2 (a^2 + 2r^2)^2 \mu'(r)) - 2\eta f^2 r \\ &\times (2a^4 + 5a^2 r^2 + 2r^4) \mu) + (a^2 + r^2) \varrho \left(\varrho' \left(2\eta f^2 (a^2 + 2r^2)^3 \mu(r) \right. \right. \\ &+ (a^2 + r^2) \left(\eta f^2 r (a^2 + 2r^2)^2 \mu'(r) + 2(a^4 (f^2 - 2r^2) + 3a^2 r^2 (f^2 \right. \\ &- 2r^2) + 4f^2 r^4 - 6r^6)) \Big) + 2r (a^4 + 3a^2 r^2 + 2r^4) \varrho'' (\eta f^2 (a^2 + 2r^2) \\ &\times \mu(r) + (a^2 + r^2) (f^2 - r^2)) \Big) - f^2 r (a^4 + 3a^2 r^2 + 2r^4)^2 \varrho(r) V(\varrho) \Big), \end{aligned}$$

The closely linked features of intricate astrophysical objects lead to complex behavior. Thus, it is difficult to determine the outcome of a slight change in any of the state determinants. For this purpose, it is convenient to formulate a complexity factor that combines the essential properties of a spherical

system in a single equation. Recently, Herrera [50] evaluated complexity of anisotropic static as well as dynamical spheres via structure scalars. These scalars were determined by splitting the Riemann tensor orthogonally. This technique is based on the assumption that the complexity reduces to zero if the fluid distribution is isotropic and homogeneous in nature. The same scheme was adopted to compute a complexity factor for static sphere in the presence of a massive scalar field [51]. This factor is defined in terms of the following structure scalar

$$Y_{TF} = Y_{TF}^{(m)} + Y_{TF}^{\varrho} = \frac{\Delta}{\varrho} - \frac{1}{2r^3} \int_0^r r^3 T_0^{0'(\text{eff})} dr - \frac{e^{-\phi_2} \varrho'}{2r\varrho}, \quad (37)$$

which effectively describes how Tolman mass (m_T) corresponding to the anisotropic sphere deviates from that of an isotropic system (provided $\Delta \neq 0$ and $\frac{d\varrho}{dr} \neq 0$) as

$$m_T = (m_T)_{\Sigma} \left(\frac{r}{r_{\Sigma}} \right) + r^3 \int_r^{r_{\Sigma}} \frac{e^{\frac{\phi_1 + \phi_2}{2}}}{r} (-Y_{TF}^{(m)} + Y_{TF}^{\varrho}) + \frac{e^{\frac{\phi_1 - \phi_2}{2}} \varrho'}{2r\varrho} dr.$$

It must be noted that a complexity-free matter source may not be isotropic and homogeneous. In the current scenario, decoupling the complexity factor via Eq.(11) leads to

$$\begin{aligned} Y_{TF} &= \frac{p_{\perp} - p_r}{\varrho} - \frac{1}{2r^3} \int_0^r r^3 (\rho' + T_0^{0'\varrho}) dr - \frac{\lambda \varrho'}{2r\varrho} \\ &+ \frac{\Theta_1^{1(\text{eff})} - \Theta_2^{2(\text{eff})}}{\varrho} - \frac{1}{2r^3} \int_0^r r^3 \Theta_0^{0'(\text{eff})} dr - \frac{\eta \mu \varrho'}{2r\varrho}. \end{aligned} \quad (38)$$

The complexity factor can be split into two components \hat{Y}_{TF} and Y_{TF}^{Θ} which define the complexity of original and additional sources, respectively as

$$\begin{aligned} \hat{Y}_{TF} &= \frac{p_{\perp} - p_r}{\varrho} - \frac{1}{2r^3} \int_0^r r^3 (\rho' + T_0^{0'\varrho}) dr - \frac{\lambda \varrho'}{2r\varrho}, \\ Y_{TF}^{\Theta} &= \frac{\Theta_1^{1(\text{eff})} - \Theta_2^{2(\text{eff})}}{\varrho} - \frac{1}{2r^3} \int_0^r r^3 \Theta_0^{0'(\text{eff})} dr - \frac{\eta \mu \varrho'}{2r\varrho}. \end{aligned}$$

Thus, in the context of SBD gravity, the complexity factor of two matter distributions existing within a static sphere is the sum of their individual complexity factors.

In order to extend the solution corresponding to Tolman IV metric functions, we impose the following constraint on complexity of the additional source

$$Y_{TF}^{\Theta} = 0, \quad (39)$$

which implies that the new source does not contribute to the complexity of the seed distribution. The above condition, corresponding to the current setup, turns out to be

$$\frac{\eta}{r(a^2 + r^2)\varrho(r)} \left(r(a^2 + r^2) \left(r^3(a^2 + 2r^2) - (a^2 + r^2)\varrho(r) \right) \mu'(r) + \mu(r) \right. \\ \left. \times \left(r^3 \left(r(a^2 + r^2)^2 \varrho' - 2(a^4 + 2a^2r^2 + 2r^4) \right) - (a^2 + r^2)^2 \varrho \right) \right) = 0. \quad (40)$$

Numerical solutions of Eqs.(10) and (40) for $\eta = 0.2, 0.5, 1$ with the initial conditions $\varrho(0) = 0.25$ and $\mu(0) = 0$ determine the corresponding scalar field and deformation function, respectively. Table 2 includes the values of ω_{BD} and other important parameters. We graphically analyze physical characteristics of solution II using the mass and radius of PSR J1614-2230. Figure 6 displays the well-behaved metric function after the transformation. The energy density and pressure components, presented in Figure 7, attain maximum values at the center and remain positive throughout the stellar interior. The anisotropy increases for some distance and then decreases towards the boundary. Moreover, all state parameters vary directly with the decoupling parameter. The considered system represents a viable distribution as it complies with all the energy bounds (refer to Figure 8). Figure 9 shows that mass, compactness and redshift increase with the radial coordinate. Further, compactness and redshift parameters obey the corresponding upper limits. Figure 10 indicates that the extended solution is consistent with causality condition as well as cracking approach. Thus, the stellar model corresponding to solution II is viable and stable for chosen values of the decoupling parameter.

5 Discussion

In this paper, we have generated new solutions representing self-gravitating models in the framework of SBD gravity. For this purpose, we have considered a static sphere in which two matter distributions (anisotropic seed and additional sources) coexist. Decoupling via MGD approach has been applied

Table 2: Values of physical parameters in solution II corresponding to $\eta = 0.2, 0.5, 1$.

	$\eta = 0.2$	$\eta = 0.5$	$\eta = 1$
ω_{BD}	9.87	10	10.2
ρ_c (gm/cm^3)	9.398×10^{15}	1.202×10^{15}	1.240×10^{15}
ρ_s (gm/cm^3)	2.008×10^{15}	2.6×10^{15}	2.6×10^{15}
p_c ($dync/cm^2$)	1.754×10^{36}	2.268×10^{36}	2.435×10^{36}
Z_s	0.057	0.072	0.072

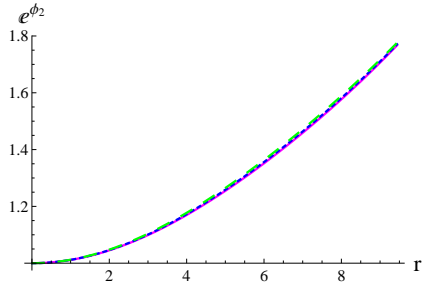


Figure 6: Behavior of deformed radial metric function for solution II.

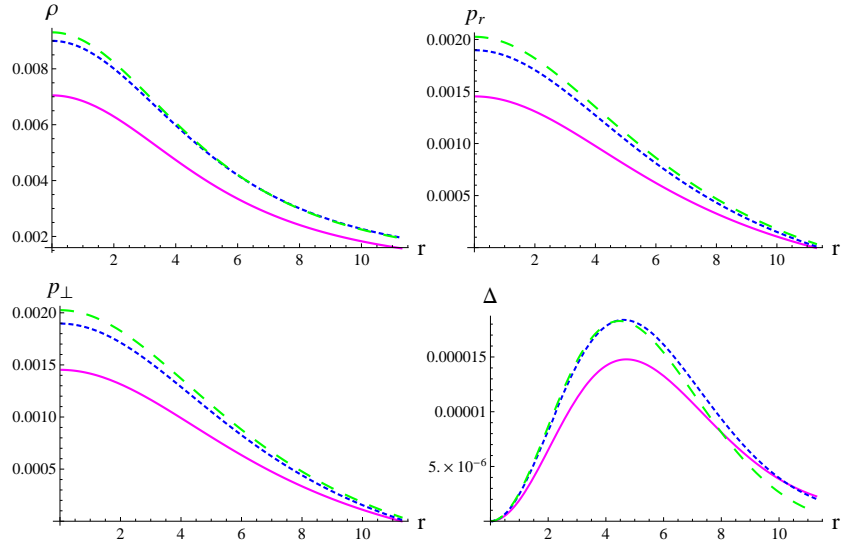


Figure 7: Behavior of ρ , p_r , p_{\perp} (in km^{-2}) and Δ for solution II.

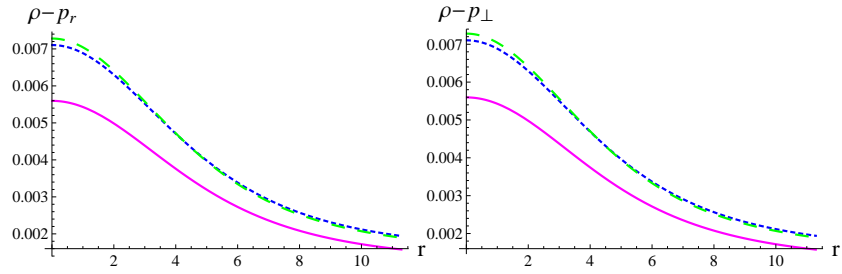


Figure 8: DEC for extended solution II.

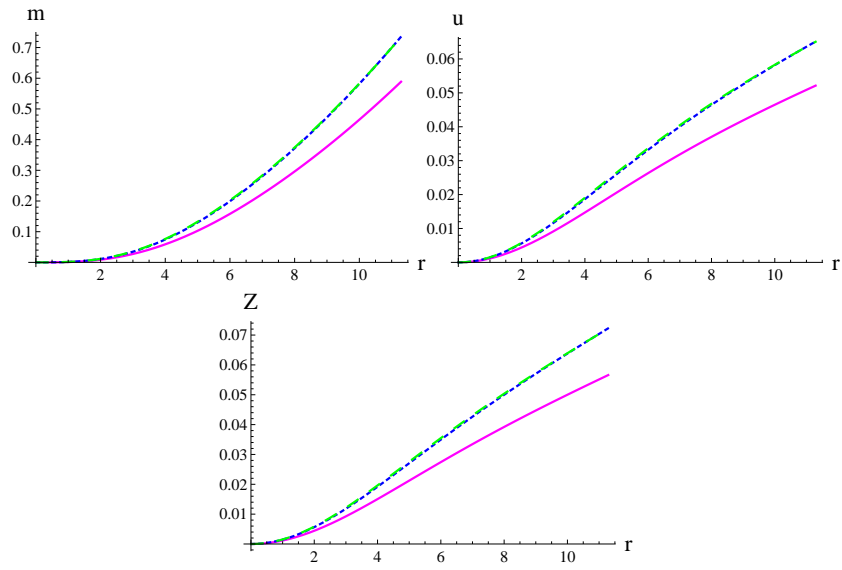


Figure 9: Behavior of m , u and Z corresponding to solution II.

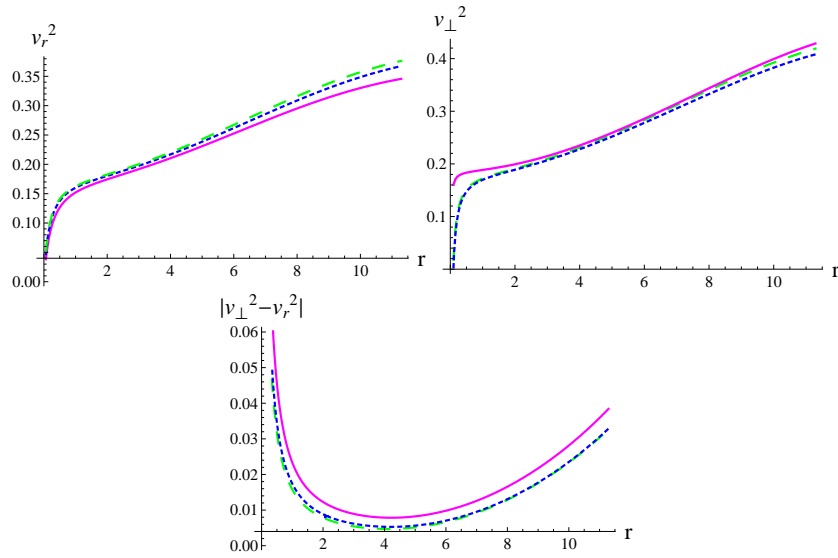


Figure 10: Plots of radial/tangential velocities and $|v_{\perp}^2 - v_r^2|$ of extended solution II.

to disintegrate the SBD field equations into two sets. The influence of the anisotropic source is limited to the first array while the second system exclusively incorporates the properties of the additional source. We have used the ansatz $\phi_1(r) = \ln\left(B^2\left(\frac{r^2}{A^2} + 1\right)\right)$, $\lambda(r) = \left(\frac{A^2+r^2}{A^2+3r^2}\right)$ and metric potentials of Tolman IV to specify the first system for solutions I and II, respectively. Solution I has been obtained by applying the condition $p_{\perp} - p_r = -(\Theta_1^1 - \Theta_2^2)$ to construct isotropic version of the original source. On the other hand, we have constructed the second solution by assuming that the complexity of the additional source is zero. These conditions have been solved numerically alongside the wave equation to evaluate the deformation function and scalar field. Moreover, the matching of internal and external spacetimes has specified the unknown constants. Finally, the behavior of obtained models has been checked via viability and stability criteria for $V(\varrho) = \frac{1}{2}m_{\varrho}^2\varrho^2$ with $m_{\varrho} = 0.01$.

We have analyzed the constructed solutions graphically for $\eta = 0.2, 0.5, 1$ by employing the mass and radius of PSR J1614-2230. The geometric transformation in the radial metric potential corresponding to solutions I and II has produced regular stellar models free from any singularity. The pressure components and energy density decrease away from the center for both solu-

tions. The matter variables related to solution II increase for higher values of the decoupling parameter whereas the first stellar model achieves maximum density and pressure for $\eta = 0.5$ and 0.2 , respectively. Moreover, we have observed that the anisotropy of the first solution is negative for $\eta = 0.2$. Thus, the stellar model possesses outward repulsive force for $\eta = 0.5$ only. On the other hand, the anisotropy of solution II is positive for the considered values of the parameters. However, it decreases towards the surface indicating a weak repulsive force near the boundary. Furthermore, both spherical structures are viable as they obey the energy constraints.

The mass, compactness and redshift parameters attain maximum values for $\eta = 0.2$ and 1 in solutions I and II, respectively. However, they do not cross their respective upper bounds in any configuration. The isotropization of the anisotropic solution is stable for $\eta = 0.5, 1$ while the second self-gravitating model agrees with the considered stability criteria (causality and cracking approach) for all three values of the decoupling parameter. Thus, it is concluded that the technique of decoupling can be applied to obtain simplified versions of complex solutions in the background of SBD theory. Moreover, the constraint $Y_{TF}^{\Theta} = 0$ has yielded viable as well as stable stellar systems for a wider range of the decoupling parameter as compared to the first solution. It is interesting to mention here that the obtained results reduce to GR for $\varrho = \text{constant}$ and $\omega_{BD} \rightarrow \infty$.

Acknowledgement

One of us (AM) would like to thank the Higher Education Commission, Islamabad, Pakistan for its financial support through the *Indigenous Ph.D. Fellowship, Phase-II, Batch-VI*.

Data availability: No new data were generated or analyzed in support of this research.

References

- [1] Dirac, P.A.M.: Nature **139**(1937)323; *ibid.* 1001; Proc. Roy. Soc. A **154**(1938)199.
- [2] Brans, C. and Dicke, R.H.: Phys. Rev. **124**(1961)3.

- [3] Will, C.M.: Living Rev. Rel. **4**(2001)4.
- [4] Weinberg, E.J.: Phys. Rev. D **40**(1989)3950.
- [5] Khoury, J. and Weltman, A.: Phys. Rev. D **69**(2004)044026.
- [6] Perivolaropoulos, L.: Phys. Rev. D **81**(2010)047501.
- [7] Buchdahl, H.A.: Int. J. Theor. Phys. **6**(1972)407.
- [8] Bruckman, W.F. and Kazes, E.: Phys. Rev. D **16**(1977)261.
- [9] Bruckman, W.F. and Kazes, E.: Phys. Rev. D **16**(1977)269.
- [10] Singh, T. and Rai, L.N.: Gen. Relat. Gravit. **11**(1979)37.
- [11] Krori, K.D. and Bhattacharjee, D.R.: J. Math. Phys. **23**(1982)1846.
- [12] Yazadjiev, S.S., Doneva, D.D. and Popchev, D.: Phys. Rev. D **93**(2016)084038; Staykov, K.V. et al.: Eur. Phys. J. C **78**(2018)586; Popchev, D. et al.: Eur. Phys. J. C **79**(2019)178.
- [13] Doneva, D.D. and Yazadjiev, S.S.: J. Cosmol. Astropart. Phys. **11**(2016)019.
- [14] Sharif, M. and Majid, A.: Eur. Phys. J. Plus **135**(2020)558; Universe **6**(2020)8.
- [15] Sharif, M. and Saba, S.: Eur. Phys. J. C **78**(2018)921; Sharif, M. and Waseem, A.: Ann. Phys. **405**(2019)14; Chin. J. Phys. **60**(2019)426; Sharif, M. and Majid, A.: Astrophys. Space Sci. **365**(2020)42; Chin. J. Phys. **68**(2020)406; Phys. Dark Universe **30**(2020)100610.
- [16] Schwarzschild, K.: Math. Phys. **189**(1916).
- [17] Ovalle, J.: Phys. Rev. D **95**(2017)104019.
- [18] Ovalle, J.: Phys. Lett. B **788**(2019)213.
- [19] Ovalle, J.: Mod. Phys. Lett. A **23**(2008)3247.
- [20] Ovalle, J. and Linares, F.: Phys. Rev. D **88**(2013)104026.

- [21] Casadio, R., Ovalle, J. and da Rocha, R.: *Class. Quantum Grav.* **32**(2015)215020.
- [22] Ovalle, J. et al.: *Eur. Phys. J. C* **78**(2018)122.
- [23] Gabbanelli, L., Rincon, A. and Rubio, C.: *Eur. Phys. J. C* **78**(2018)370.
- [24] Estrada, M. and Tello-Ortiz, F.: *Eur. Phys. J. C* **133**(2018)453.
- [25] Sharif, M. and Sadiq, S.: *Eur. Phys. J. C* **78**(2018)410.
- [26] Panotopoulos, G. and Rincon, A.: *Eur. Phys. J. C* **78**(2018)851.
- [27] Gabbanelli, L. et al.: *Eur. Phys. J. C* **79**(2019)486.
- [28] Contreras, E.: *Class. Quantum Grav.* **36**(2019)095004.
- [29] Contreras, E. and Bargueno, P.: *Class. Quantum Grav.* **36**(2019)215009.
- [30] Casadio, R. et al.: *Eur. Phys. J. C* **79**(2019)826.
- [31] Hensh, S. and Stuchlik, Z.: *Eur. Phys. J. C* **79**(2019)834.
- [32] Singh, K.N. et al.: *Eur. Phys. J. C* **79**(2019)851.
- [33] Sharif, M. and Ama-Tul-Mughani, Q.: *Int. J. Geom. Methods Mod. Phys.* **16**(2019)1950187; *Mod. Phys. Lett. A* **35**(2020)2050091.
- [34] Cedeño, F.X.L. and Contreras, E.: *Phys. Dark Universe* **28**(2020)100543.
- [35] Tello-Ortiz, F. et al.: *Chin. Phys. C* **44**(2020)105102.
- [36] da Rocha, R: *Symmetry* **12**(2020)508.
- [37] da Rocha, R: *Phys. Rev. D* **102**(2020)024011.
- [38] Contreras, E., Ovalle, J. and Casadio, R.: *Phys. Rev. D* **103**(2021)044020.
- [39] Contreras, E. and Fuenmayor, E.: *Phys. Rev. D* **103**(2021)124065.
- [40] Sultana, J.: *Symmetry* **13**(2021)1598.

- [41] Faraoni, V.: *Class. Quantum Grav.* **26**(2009)145014; Yazadjiev, S.S., Doneva, D.D. and Popchev, D.: *Phys. Rev. D* **93**(2016)084038; Motahar, Z.A. et al.: *Phys. Rev. D* **96**(2017)064046; Staykov, K.V. et al.: *Eur. Phys. J. C* **78**(2018)586; Fattoyev, F.J.: *Arab. J. Math.* **8**(2019)293; Danchev, V.I. and Doneva, D.D.: *Phys. Rev. D* **103**(2021)024049.
- [42] Santos, C. and Gregory, R.: *Ann. Phys.* **258**(1997)111.
- [43] Quiros, I.: *Int. J. Mod. Phys. D* **28**(2019)7.
- [44] Fattoyev, F.J.: Kase R. and Tsujikawa, S.: *J. Cosmol. Astropart. Phys.* **09**(2019)054; Maurya, S.K. et al.: arXiv:2008.10600.
- [45] Einstein, A.: *Ann. Math.* **40**(1939)922.
- [46] Fujii, Y. and Maeda, K.: *The Scalar-Tensor Theory of Gravitation* (Cambridge University Press, 2003).
- [47] Buchdahl, H.A.: *Phys. Rev. D* **116**(1959)1027.
- [48] Ivanov, B.V.: *Phys. Rev. D* **65**(2002)104011.
- [49] Tolman, R.C.: *Phys. Rev.* **55**(1939)364.
- [50] Herrera, L.: *Phys. Rev. D* **97**(2018)044010.
- [51] Sharif, M. and Majid, A.: *Chin. J. Phys.* **61**(2019)38.